Chapter 2

Seismic waves in random media

The earth's interior is heterogeneous and can only to a certain degree be described by simple physical models. Tectonic, climatic, petrophysical, geothermal and other factors have build up a complex structure that contains heterogeneities over all scales, from several centimeters up to tens of kilometers. One way to describe this medium is to consider it as a random medium with spatial statistical distributions of its physical properties, e.g. P- and S-wave velocities, density.

In the following, an introduction to random media and their statistical descriptions will be given. In the second part an overview on scattering regimes and related phenomena will be given. The effects of scattering on seismic imaging will be discussed and further aspects with importance to seismic imaging will be considered.

2.1 Statistical description of random media

The velocity field of a heterogeneous medium can be described as a superposition of a deterministic part v_0 (mean velocity) and a fluctuating part $\delta v(\vec{x})$:

$$v(\vec{x}) = v_0 + \delta v(\vec{x}) = v_0(1 + \xi(\vec{x})) \tag{2.1}$$

where $\vec{x}$ is the spatial position vector. $\xi(\vec{x})$ is the fractional fluctuation of the velocity. The mean velocity v_0 is chosen such that:

$$v_0 = \langle v(\vec{x}) \rangle \text{ and } \langle \xi(\vec{x}) \rangle = 0,$$

i.e. v_0 equals the average velocity in the medium and the mean fluctuation is zero. $\langle ... \rangle$ denotes the ensemble average.

The autocorrelation function (ACF) is then defined as:

$$F(\vec{x}) = \langle \xi(\vec{y})\xi(\vec{y}+\vec{x}) \rangle, \tag{2.2}$$

with the so called lag distance $\vec{x}$. The ACF is a statistical measure of the spatial correlation and the magnitude of the fluctuations in the medium. It describes the degree of similarity of the medium's parameters in dependence on the lag distance $\vec{x}$. When the medium is isotropic, the ACF depends only on $r = \mid \vec{x} \mid$. The magnitude of the velocity fluctuations is given by the mean square of the fractional fluctuation:

$$\epsilon^2 \equiv F(\vec{0}) = \langle \xi(\vec{x})^2 \rangle \tag{2.3}$$

with the variance ϵ^2 and the standard deviation ϵ. The spatial variation of the fluctuations is characterised by the correlation length a. The Fourier transform of the correlation function provides the power spectral density function (PSDF),

$$P(\vec{k}) = \int_{-\infty}^{\infty} \int_{-\infty}^{\infty} \int_{-\infty}^{\infty} F(\vec{x}) e^{i\vec{k}\vec{x}} d\vec{x} \tag{2.4}$$

with the wave number vector $\vec{k}$.

Three correlation functions are commonly used: the Gaussian, the von-Kármán and the exponential correlation function. The correlation functions and their corresponding PSDFs are given in Tab. 2.1. The Gaussian correlation function describes a low-pass filtered white noise. This function is poor in short wavelength components and thus too smooth to represent the heterogeneities in the earth. A more accurate description when modelling the earth's interior is given by the von-Kármán correlation function. It describes a self-similar and self-affine medium and is rich of short wavelength components. It provides a fractal spatial description of a fabric over a wide scale range, and is commonly used to model geological structures. When the Hurst number becomes $\kappa = 0.5$ $(0 \leq \kappa \leq 1)$, then the von-Kármán function coincides exactly with the exponential function. In Gaussian and exponential media the correlation length a is directly related to the dominant characteristic scale lengths of the heterogeneities in the medium.

In Fig. 2.1(a) Gaussian and exponential autocorrelation functions are plotted, normalised to the variance and to the correlation length. Both correlation functions decrease to $\frac{1}{e}$ of their maximum at the lag distance equal to the correlation length in the medium.

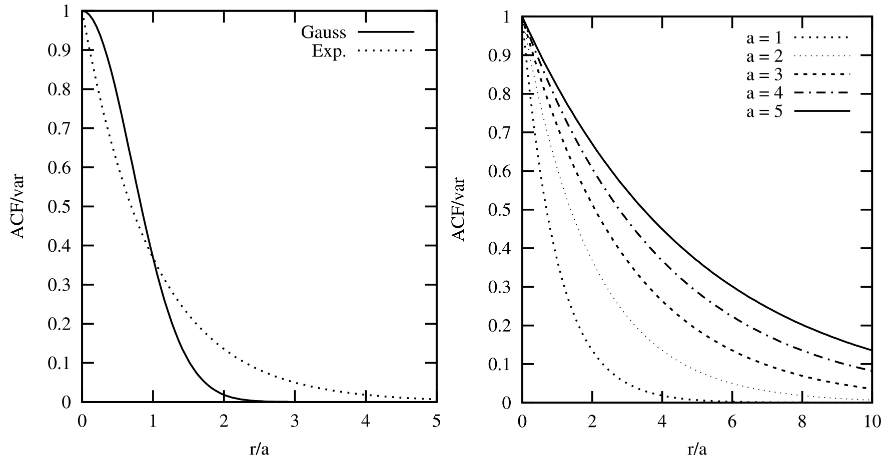

(a) (b)

Figure 2.1: (a) Gaussian and exponential autocorrelation functions, normalised to the lag and the variance of the medium. (b) Exponential autocorrelation functions with different correlation lengths.

The slope of the correlation functions depends on the correlation lengths of the medium Fig. 2.1(b).

Typ	**ACF**	$\mathbf{P}(k)$
Gauss	$F(r) = \epsilon^2 e^{-r^2/a^2}$	$P(k) = \epsilon^2 a^3 \sqrt{\pi^3} e^{-k^2 a^2/4}$
Exponential	$F(r) = \epsilon^2 e^{-r/a}$	$P(k) = \frac{8\pi\epsilon^2 a^3}{(1+k^2a^2)^2}$
von-Kármán	$F(r) = \frac{\epsilon^2 2^{1-\kappa}}{\Gamma(\kappa)} \left(\frac{r}{a}\right)^\kappa K_\kappa \left(\frac{r}{a}\right)$	$P(k) = \frac{8\epsilon^2 \pi^{3/2} a^3 \Gamma(\kappa+3/2)}{\Gamma(\kappa)(1+k^2a^2)^{\kappa+\frac{3}{2}}}$

Table 2.1: Autocorrelation functions and their power spectral density functions in 3D. Γ is the gamma function, K_κ the modified Bessel function of second kind of order κ, and κ the Hurst number.

A random medium realisation is obtained by calculation of a white noise spectrum. This spectrum is filtered with the square root of the PSDF of the correlation function in the wavenumber domain. The inverse Fourier transformation provides the fluctuation field which is superposed on the homogeneous background. Examples of Gaussian, exponential

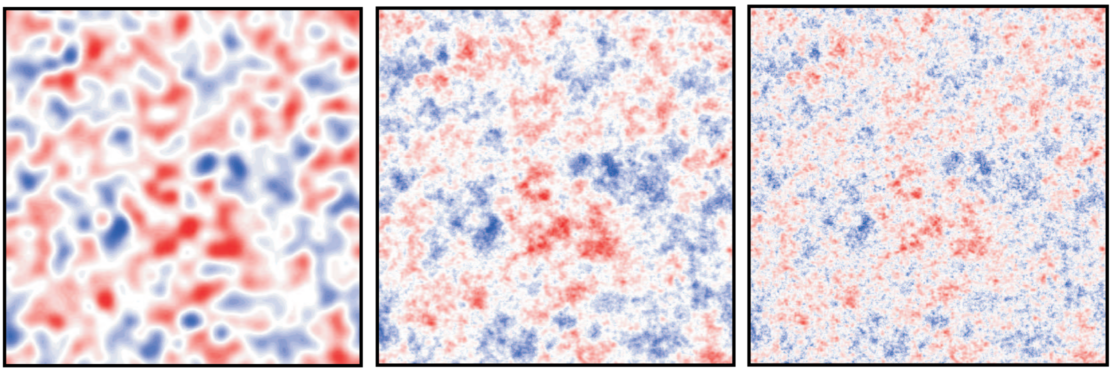

(a) (b) (c)

Figure 2.2: Examples of random media realisations with (a) Gaussian, (b) exponential and (c) von-Kármán autocorrelation function (Sick, 2002).

and von-Kármán media realisations are shown in Fig. 2.2. The Gaussian medium appears smooth, compared to the von-Kármán and the exponential medium, which appear rough due to short wave length components of the heterogeneities.

2.2 Wave phenomena in random media

Seismic waves that propagate through heterogeneous media are affected by amplitude and phase fluctuations due to scattering. Scattering occurs due to the interaction of the seismic wave field with the heterogeneities in the medium. Commonly scattering regimes are classified into Rayleigh, Mie and forward scattering. Introduction to the regimes and scattering phenomena will be given in the following.

2.2.1 Scattering regimes

The amount of scattering interaction between the seismic wave and the heterogeneities depends on the relative size of the heterogeneity a compared to the dominant wavelength λ of the seismic wave. A dimensionless parameter $k \cdot a$ (with the wave number $k = \frac{2 \cdot \pi}{\lambda}$) is introduced. $k \cdot a$ is referred to as the normalised wave number describing the relative correlation length with respect to the seismic wavelength. The following scattering regimes can be described:

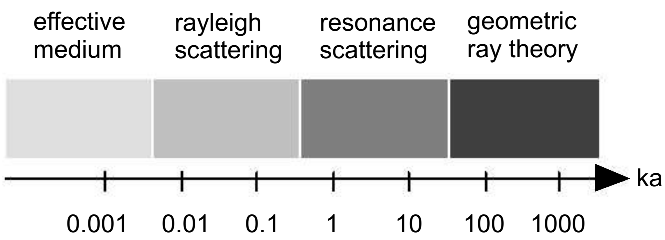

Figure 2.3: The scattering regimes. The magnitude and the radiation characteristics of the scattering is controlled by the product of the wavenumber k and the radius of the scatterer a (from Pyrak-Nolte (2002)).

Quasi-homogeneous and effective medium regime: $k \cdot a < 0.01$. The seismic medium can be regarded as quasi-homogeneous, because the heterogeneous scale lengths are small compared to the seismic wavelength. Scattering effects are negligibly small.

Rayleigh scattering regime: $0.01 \leq k \cdot a < 0.1$. Considering weak fluctuation of the elastic parameters, Rayleigh scattering can be described using the Born approximation, which is based on the single scattering assumption. The amount of scattered energy in 3D is proportional to k^4, leading to apparent attenuation of high frequencies.

Mie scattering regimes: $0.1 \leq k \cdot a \leq 10$. In the Mie scattering regime, also known as resonant scattering, heterogeneity scale lengths are in the order of the seismic wavelength. The incident waves are scattered with large angles relative to the incident direction (*large angle scattering*) and a reflection coda can be observed in the wave field.

Forward scattering regime: $10 \leq k \cdot a$. The seismic wavelength is small compared to the correlation lengths and the seismic energy is scattered mainly in the forward direction. Backscattering is small and focusing, diffraction and interference effects become important.

In the **forward scattering** regime three sub-regimes can be classified depending on the scattering strength and the diffraction type. Two additional dimensionless parameters are introduced (Flatté et al., 1979; Aki and Richards, 1980): the *diffraction parameter* Λ and Φ, which describes the scattering strength. The diffraction parameter Λ describes the size and the spatial extent of the heterogeneities with respect to the first Fresnel zone:

$$\Lambda \approx (\frac{R_{Fr}}{a_h})^2 \tag{2.5}$$

with R_{Fr} the radius of the zero-offset Fresnel zone and a_h the correlation length orthogonal to the wave propagation direction. Small values for $\Lambda < 1$ correspond to a backscattered field that is dominated by specular reflection, whereas larger values characterise a wave field that is dominated by diffraction. The scattering strength Φ is dependent on the fluctuation of the velocity field ϵ, the travel path L, the integral scale length of the impedance field a_i, and the characteristic wave number k_0:

$$\Phi = k_0 \cdot \epsilon \sqrt{L \cdot a_i} \tag{2.6}$$

The so called integral scale length can be approximated by $a_i = 0.4 \cdot a_v$ with the correlation length parallel to the propagation direction a_v. The two parameters characterise the four sub-domains of forward scattering, i.e *specular reflection or ray theory, diffraction, weak scattering and strong scattering* (Fig. 2.4). By transferring data parameter onto this map an estimate of the scattering regimes of the actual scattering regimes is given.

Generally one can say that scattering phenomena become strong when correlation lengths of heterogeneous structures are in the order of the dominant wavelength and when travel paths become large (Mavko et al., 1996). A brief overview and references to literature of methods to describe weak and strong fluctuation regimes e.g. Born, Bourret, Rytov, Markov and other approximations are given in Müller (2001).

Regarding the numerical experiments in this thesis the following scattering parameters are expected: The frequency range of the synthetic data is between 5 - 30 Hz, the maximum travel distance is about 140 km. The correlation lengths in the heterogeneous layer varies between hundreds of meters up to several kilometres (500 - 6000 m), and the standard deviation varies between 1 % - 20 %. This provides the following parameter ranges for the diffraction parameter and the scattering strength parameter: $0.6 \leq \Lambda \leq 6$ and $0.3 \leq \Phi \leq 5$. These parameters approximately describe the setting of the deep reflection data processed in this thesis. Transfer of these values onto the map (Fig. 2.4, (b)) yields that specular reflection, weak and strong scattering as well as diffraction have to be expected in the data. Thus, the reflection phenomena observed in the deep reflection data processed in this thesis cannot be classified by only one type, but several regimes have to be considered.

A short introduction to some important amplitude and phase phenomena related to the wave propagation through heterogeneous media will be given in the following.

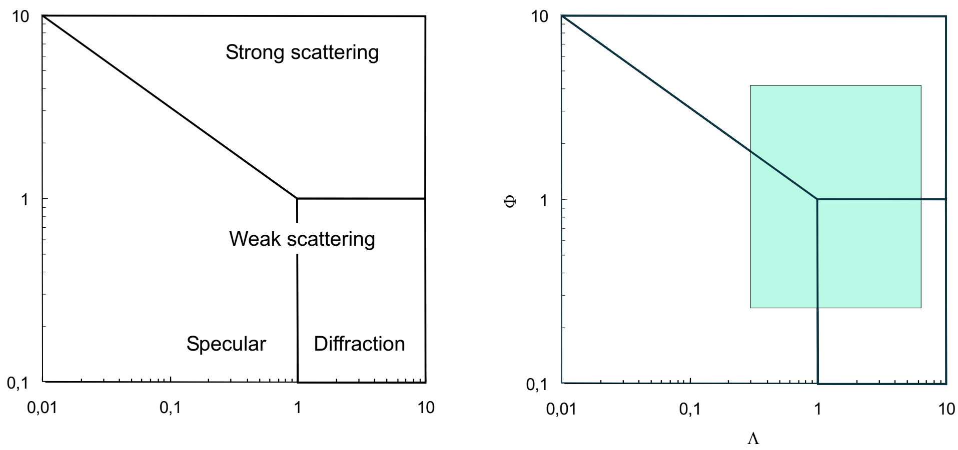

(a) (b)

Figure 2.4: (a) Scattering regimes in the $\Lambda - \Phi$ space (after Flatté et al. (1979)). (b) Estimated scattering field for the ANCORP experiment marked by the blue box.

2.2.2 Amplitude and phase in heterogeneous media

Seismic images are affected by amplitude and phase fluctuations of waves travelling trough heterogeneous media. Some of these phenomena are introduced in the following.

Seismic waves that travel through an elastic medium suffer from attenuation of seismic energy. The attenuation rate is a sum of scattering (the redistribution of seismic energy) and intrinsic attenuation (the conversion of seismic energy into heat). It was observed that in general scattering attenuation is the dominant factor for attenuation in the crust (Hatzidimitriou, 1995; Del Pezzo et al., 1995). Both, scattering and intrinsic attenuation are frequency dependent. In general, the attenuation rate increases for higher frequencies. However, theoretically and numerically estimated scattering attenuation rates for Gaussian, von-Kármàn and exponential media showed that scattering attenuation rate is not only dependent on the frequency, but also on the medium parameters (Raynaud, 1988; Sato and Fehler, 1998; Yoshimoto et al., 1998; Hong, 2004). Scattering of seismic waves causes amplitude attenuation and phase fluctuations. Reflection images are affected by these phenomena, especially, if the target is located beneath strongly heterogeneous media, e.g. in sub-salt, sub-basalt or crustal imaging. Even if impedance contrasts are large reflections from structures located below are hardly revealed. Seismic amplitudes are also influenced by focusing and defocusing due to ray bending caused by weak velocity

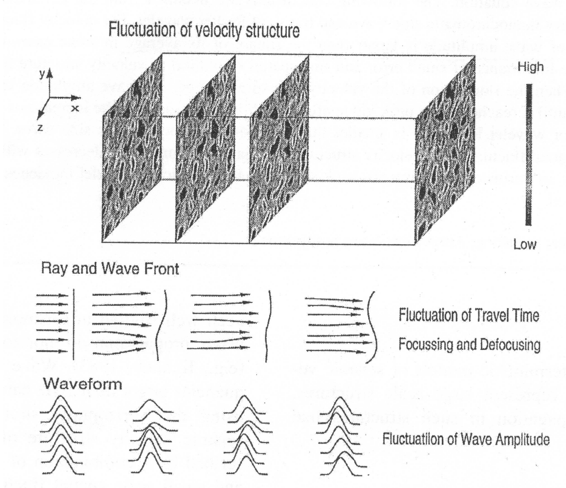

Figure 2.5: Schematic sketch showing wave propagation through random media (from Hoshiba (2000)). Rays tend to bend when facing heterogeneities in the medium, causing focusing and defocusing resulting in amplitude fluctuations.

fluctuations in the medium (Fig. 2.5). These effects cause large amplitude fluctuations, i.e. locally higher and smaller wave amplitudes. Results from numerical studies showed that the amplitude fluctuations increase with the propagation distance, until they reach a maximum, and decrease afterwards (Hoshiba, 2000). Also, the frequency dependence of reflectivity and the transmissivity in randomly layered media affects the seismic amplitudes (Shapiro and Hubral, 1999; Imhof, 2003).

The traveltimes of waves in random media are also affected by the heterogeneities in the medium. Constant phase retardation of the transmitted field is observed if components are scattered through very small angles (forward scattering). Also, lateral variations in the phase and the amplitudes of the primary field reducing the lateral coherence occure if the scattering angles are slightly larger (Sato, 1982a,b). Results from numerical modelling showed that the incoherency of the wave field rapidly increases with increasing frequency (Raynaud, 1988). From ray-theoretical considerations it was revealed that the magnitude of the phase variations are proportional to the variance of the velocity fluctuations in the medium, the correlation length of the heterogeneities and the propagation distance (Roth, 1997). Numerical studies revealed that the variance of travel time fluctuations decreases with increasing offsets at small offsets (Iooss, 1998), while theoretical considerations showed that the variance of travel time fluctuations increases again after a critical distance (Kravtsov et al., 2003).

Besides the traveltime fluctuations the so called velocity shift is an important phenomenon in heterogeneous media. According to Fermat's principle seismic waves travel along the fastest ways through the medium. The traveltimes of these waves are smaller than for waves travelling with the corresponding average velocity of the medium. Thus, the velocities derived from analysis of reflection data are shifted towards values higher than the average velocity values of the medium. The velocity shift is proportional to the variance of the velocity fluctuations in the medium and increases with decreasing ratio between the wavelength and the correlation length of the heterogeneities λ/a (Roth, 1996). For larger wavelengths ($\lambda/a \geq 4$) the velocity shift becomes small. The velocity shift shows similar frequency dependent behaviour with dispersion due to anelasticity which is of seismological relevance (Müller et al., 1992). The velocity shift of teleseismic body waves can be around 0.2 %, while it is negligible small for teleseismic surface waves. This velocity dispersion, which is of similar amount as the dispersion due to anelasticity, provides an alternative explanation for the observed traveltime difference between short period body waves and long period surface waves of teleseismic events. For velocity fluctuations of a few per cent the velocity shift is considerably small, such that corrections of the observed velocities are not required for reflection seismic problems (Müller et al., 1992).

First theoretical considerations on reflection amplitudes in random media are given by O'Doherty and Anstey (1971), who studied the effects of stratigraphic filtering on reflection amplitudes, pulse broadening and delaying effects of the coda. A selection of later studies on seismic transmission and amplitude effects due to multiple scattering is given by Shapiro and Kneib (1993), Shapiro and Hubral (1999), Douma and Roy-Chowdhury (2001), Herman (2001), and Imhof (2003). For a comprehensive overview on seismic scattering the reader is referred to Wu and Aki (1988), Ishimaru (1997), and Sato and Fehler (1998). Further studies on traveltimes in random media concerning different aspects, e.g. velocity shift, phase velocity, velocity dispersion and statistics were presented by Spetzler and Snieder (2001), Baig et al. (2003), Roth et al. (1993), Roth (1996), Marion et al. (1994), and Kravtsov et al. (2003).

2.3 Factors affecting seismic images

The amplitude and phase fluctuations introduced in the previous section influence the reflectivity and the coherency of seismic images in heterogeneous media. In the following other factors that can have an impact on the reflection image and thus on the structural interpretation will be discussed.

One major key to seismic imaging is the derivation of an appropriate velocity model. In seismic reflection experiments the resolution of the velocity heterogeneities is limited. Deterministic methods such as velocity analysis or ray tomography cannot resolve small structures of the velocity field (Thore and Juliard, 1996; Williamson and Worthington, 1993). Commonly the lateral resolution is the size of the first Fresnel zone. In deep seismic imaging the Fresnel zone becomes several kilometers, such that heterogeneities of shorter scales will hardly be detected. But also larger heterogeneities with no sharp discontinuities will not cause significant reflections while affecting the seismic travel times (Jannane et al., 1989).

Besides the limited resolution, anisotropy, i.e. dependence of the seismic velocity on the propagation direction, can play an important role in the velocity analysis using seismic data. Anisotropy can be caused by preferred mineral orientation of the rocks or due to layering of isotropic solids. The seismic response to both models remains the same. In both cases the waves travel faster in one direction compared to the other direction. Oriented cracks or aligned inclusions as well as finely layered structures render seismic records anisotropic without causing reflections and remain unrecognised (Weiss et al., 1999; Folstad and Schoenberg, 1992). The correlation lengths, the aspect ratios, i.e. the ratio between the width and the height of the heterogeneities, and the degree of anisotropy determined from real data analysis show a large variety. For example Dolan et al. (1998) proposed that the correlation lengths in the upper crust are in the order of kilometers with aspect ratios of about 4. Other studies derived aspect ratios for the upper crust smaller than 2 (Wu et al., 1994), and aspect ratios between 2 - 5 and correlation lengths of 400 - 1000 m (Levander and Holliger, 1992). The amount of velocity anisotropy estimated from seismic data varies, e.g. P-wave anisotropy in the Ivrea region (Northern Italy) varies between 10 - 26 % (Burlini and Fountain, 1993), but typical values are around 5 % (Anderson, 1989). In laboratory measurements more than 10% P-wave anisotropy is frequently observed (Weiss et al., 1999).

Anisotropy of a few per cent can play an important role in deep seismic imaging. The velocity model is often obtained from refraction data recorded during the reflection seismic survey. The analysis of refraction data is indispensable if the data coverage of the reflection data sets is too low to yield reliable models from velocity analysis. The velocity models obtained from tomographic inversion often suffer from low resolution and are strongly dependent on the starting model used for the data inversion. However, refraction seismics mainly regard horizontally travelling waves. In reflection data, dominantly vertical travel paths are considered. When anisotropy is present the velocities obtained from refraction data analysis will only reveal the seismic velocity in the horizontal propagation direction.

Dependent on the subsurface structure the velocities derived from wide-angle data analysis will differ from the velocities in the vertical propagation direction. If the heterogeneities are dominantly horizontally layered, the derived velocities will be larger, in case of vertically oriented heterogeneities, the velocities obtained from refraction data will be smaller. The following example demonstrates the possible effect of anisotropy on the reflector depth: A reflection event recorded at 20 s two-way-travel time is migrated using the velocity derived from refraction data analysis. The derived velocity is 7500 ms^{-1} such that the reflection is imaged at a depth of 75 km. It is assumed that the anisotropy in the medium is about 7 % and that the velocities in the horizontal direction are slower than in the vertical direction. Thus, the corresponding velocity in the vertical propagation direction is around 8000 ms^{-1}. When using this velocity for migration the recorded reflection is imaged at a depth of 80 km. The difference in depth of both images is about 5 km. In case of stronger anisotropy (10% $\leq$) this difference becomes significantly large.

Besides the accuracy of the velocity models the imaging technique plays an important role. Migration methods can be applied either before of after stacking of the data. Post-stack migration is commonly applied to Common-Mid-Point (CMP) processed data. CMP processing has the advantage of effectively reducing the data volume and improving the signal-to-noise ratio, but the loss of amplitude information and the loss of information on fine-scale structures have to be taken into account. Especially in regions with complex subsurface basic assumptions of CMP stacking are not fulfilled, e.g. the reflectors have to be rather plane, reflections has to be rather continuous with lengths exceeding the width of the Fresnel zone and the dip of the reflector has to be rather moderate (Meissner and Rabbel, 1999). Also, the CMP stacking acts as a dip filter and decreases the horizontal resolution in the final stacked image (Yilmaz, 1987; Berkhout, 1984). Apparently it increases the horizontal coherency in the images of random heterogeneities and in some cases it causes smearing artefacts, especially for large offsets, which cannot be removed by poststack migration (Emmerich et al., 1993; Gibson and Levander, 1990; Holliger and Levander, 1992). The Kirchhoff prestack depth migration technique seems most appropriate in imaging heterogeneous media as it assumes every subsurface point as a potential scatterer. Thus, complex subsurface structures are properly imaged. Prestack migration techniques are computing intensive, but for seismic data with low coverage in strongly heterogeneous media they provide depth images of high quality, thus justifying its application. Often, the seismic images obtained from migration of 2D data sets acquired in areas with complex subsurface structures contain reflections from structures located off to the side of the acquisition line. These events are hardly recognised in the data and suppressing of these signals from the seismic records prior to further processing is difficult.

In the case of a crooked line geometry of the profile the computing expensive migration in 3D is requires to image the offline events at their true subsurface positions. Thereby, 3D migration profits from two points: the 3D images enable a structural interpretation of the reflections in 3D, and spatial noise can be significantly reduced (Sheriff and Geldart, 1995).

However, even if the image was obtained from prestack migration using the right velocity model, the interpretation of scatterers is limited. Results from numerical modelling showed that scatterers with preferred orientations cause reflection signatures that are hardly distinguishable from horizontally oriented structures (Emmerich et al., 1993). The results also revealed that multiple scattering can produce coherent arrivals in the seismograms without having real counterparts in the subsurface. Thus, reflections from strongly heterogeneous regions might only indicate the existence of a zone of heterogeneities without revealing true internal structures.

Imaging of heterogeneous regions is still a difficult task as the images are often affected by a number of different factors. Some of these factors, e.g. the influence of heterogeneous overburden on the reflections below and its impact on the image, will be studied using synthetic and real data in the following.